

Grain-size-dependent zero-strain mechanism for twinning in copper

J. Y. Zhang,¹ P. Zhang,¹ R. H. Wang,² G. Liu,^{1,*} G. J. Zhang,² and J. Sun^{1,†}

¹State Key Laboratory for Mechanical Behavior of Materials, Xi'an Jiaotong University, Xi'an 710049, China

²School of Materials Science and Engineering, Xi'an University of Technology, Xi'an 710048, China

(Received 1 March 2012; revised manuscript received 29 July 2012; published 22 August 2012)

It is generally accepted that deformation twinning in coarse-grained metals contributes the macroscopic strain, while most deformation twins in nanocrystalline (NC) metals, contrary to popular belief, yield zero net macroscopic strain via either the cooperative or random activation of all three Shockley partials. In the former, the three partials with a particular $(b_2:b_1:b_3)$ triplet unit are successively emitted, while in the latter the three partials are randomly activated in equal numbers. Here we report that there exists a transition between the two zero-strain deformation twinning mechanisms, i.e., from cooperative activation of partials to random activation of partials in NC Cu with medium stacking-fault energy, that occurs with decreasing grain size at room temperature and different strain rates. This experimental finding provides insight into the understanding of deformation twinning.

DOI: 10.1103/PhysRevB.86.064110

PACS number(s): 62.20.-x

I. INTRODUCTION

Deformation twinning¹⁻⁶ (DT) is quite an important deformation mechanism in face-centered-cubic (fcc) metallic materials, accomplished by the glide of twinning dislocations to accommodate plastic deformation under mechanical stress, especially in nanocrystalline (NC) metals. It is a tenet that the higher is the stacking-fault energy (SFE) of the fcc metals the lower is the twinning probability. For example, coarse-grained fcc metals with medium-to-high SFEs such as Cu, Al, and Ni usually prefer to deform by dislocation slip at room temperature and low strain rate ($\dot{\epsilon}$), while low-SFE metals such as Ag primarily deform by twinning. In contrast to coarse-grained fcc metals, which exhibit a Hall-Petch-type dependence for DT at low temperatures and high $\dot{\epsilon}$,^{1,7,8} NC fcc metals become easier to twin with decreasing grain size (D), reaching a maximum twinning probability, and then become more difficult to twin when grain size D decreases further, i.e., they exhibit an inverse- D effect on DT, even at room temperature and low $\dot{\epsilon}$.^{9,10}

Molecular dynamics (MD) simulations^{11,12} and experimental observations²⁻⁵ have revealed that the mechanisms of DT in NC metals are fundamentally different from those in their coarse-grained counterparts,^{1,13,14} which renders several types of deformation twins (DTs) that are exclusively observed in NC metals.¹⁵ Specifically, Wu *et al.*⁵ proposed a random activation of partials (RAP) in equal numbers of all three possible Shockley partials emitted from grain boundaries (GBs), to explain the zero-net-macrostrain deformation twinning (ZSDT) phenomena in NC metals with medium to high SFEs (Al, Ni, Cu). It is noted that since the participating Burgers vectors sum to zero in the RAP mechanism, RAP twins must produce zero net macroscopic strain. Concomitantly, GB segments are smooth even at locations intersecting the TBs, which is a characteristic signature of zero macroscopic strain.⁵ Most recently, Liu *et al.*⁶ also revealed through *in situ* high-resolution transmission electron microscope (HRTEM) observations a ZSDT mechanism via nucleation, and the migration of a $\Sigma 3\{112\}$ incoherent twin boundary in micron-sized Ag with low SFE, fundamentally different from the RAP mechanism. Since $\Sigma 3\{112\}$ incoherent twin boundaries can be present with a set of Shockley partial dislocations with

a repeatable sequence $b_2:b_1:b_3$ on every (111) plane,^{16,17} a noteworthy characteristic of the three partial dislocations is that the sum of their Burgers vectors in one triple unit equals zero.^{6,18} This cooperative activation of a particular set of $b_2:b_1:b_3$ partials as a triplet unit (CAP) mechanism, which can cause the detwinning of nanotwins,¹⁷ also introduces zero macroscopic strain in plastic deformation. It is thus very difficult to distinguish the two ZSDT mechanisms from each other in terms of the morphologies of DTs (i.e., CAP twins and RAP twins) in NC fcc metals if the two ends of the DTs terminate at GBs. However, if the DTs end in the grain interior (forming $\Sigma 3\{112\}$ incoherent twin boundaries that can dissociate into two tilt walls bounding a $9R$ phase¹⁶) the CAP twins may be discerned by the $9R$ stacking sequence $ABC/BCA/CAB$, which is equivalent to a close-packed stacking of fcc $\{111\}$ planes with an intrinsic stacking fault inserted at every third close-packed plane,^{16,17} suggesting that low SFE is a key requirement for the effect. Furthermore, the dissociated $9R$ region is not rigidly fixed, but can vary depending on external conditions (e.g., stress, time).^{19,20} For example, *in situ* HRTEM observations¹⁹ of an incoherent twin boundary in Cu demonstrated that the width of the $9R$ slab can vary with time (in this case increasing from about 1.4 nm to about 3.0 nm width), breaking the stacking from the normal $ABC/BCA/CAB$ sequence, which indicates that the $9R$ structure depends sensitively on the local state of mechanical loading. Therefore, this ordered $9R$ structure is less likely to be observed in the RAP twins as the grain configuration (or size) is changed, due to the random activation of partials. In such cases, the arrangement of faults (i.e., $9R$ structure) is sufficiently regular that one can distinguish the CAP from the RAP twins. Moreover, the experimental evidence is still insufficient concerning DT via the collective glide of incoherent twin boundaries, and the puzzle of how the grain size influences the ZSDT mechanism needs to be clarified, especially in NC metals with medium to high SFEs.

Here we report experimental observations of a grain-size effect on the ZSDT mechanism in tensile-tested NC Cu films, at room temperature. Large-sized Cu grains tend to deform via the CAP ZSDT mechanism, while small-sized Cu grains prefer to deform via the RAP ZSDT mechanism.

II. EXPERIMENTAL METHODS

Polyimide-supported 500-nm-thick Cu thin films were synthesized by means of direct current (dc) magnetron sputtering at room temperature. The as-deposited films were annealed *in situ* at 150 °C to stabilize the microstructure. X-ray diffraction showed a strong (111) peak, followed by (200) and (220) peaks, indicating that the majority of the grains have these out-of-plane orientations. The grain-size distribution was examined in a transmission electron microscope (TEM), revealing a grain-size range spanning 300 to 20 nm, as shown in Figs. 1 and 2. The samples were uniaxially stretched to ~20% total elongation at room temperature using a MTS Tytron 250 at $\dot{\epsilon} = 1 \times 10^{-4}$ /s and 1×10^0 /s. Postexperiment TEM examinations provided an estimate of the number of grains that contained DTs, following the procedures in Ref. 9. We examined ~100 grains for each grain size in each tensile-deformed specimen. Since before tensile pulling there were already some grains that contained initial growth or annealing

twins (~4%⁹), only the increment will be taken as the DTs. In other words, the number of grains containing DTs generated during deformation is then determined from the difference between the two numbers before and after deformation, and the fraction of DT-containing grains is obtained by normalizing against the total number of grains (100) at the particular grain size D (each D is for grain sizes within a 10 nm bin width). Still, one has to keep in mind that not all twins or stacking faults are visible in a plan-view TEM image. More details about the experimental and statistical procedures can be found in our previous work.⁹ To investigate the grain-size effect on the ZSDT mechanism, we further examined the fraction of DTs ended in the grain interior generated by the RAP and CAP mechanisms, respectively, at each strain rate. Here, to distinguish the RAP twins from CAP twins ending in the grain interior, we identify the characteristics of the front tips of incoherent twin boundaries through the HRTEM observations, because the front of incoherent twin boundaries of CAP twins is generally composed of the 9R phase and has two phase

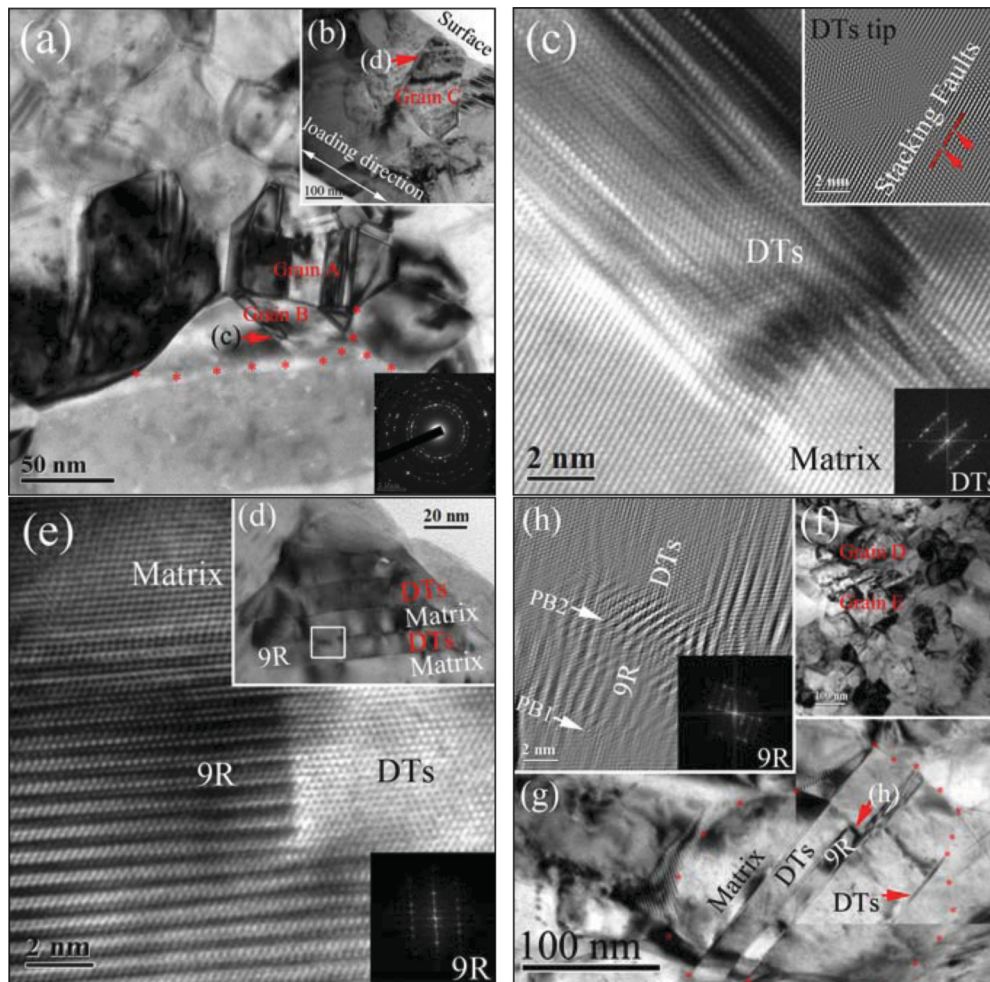


FIG. 1. (Color online) (a), (f) Plan-view and (b) cross-sectional TEM micrographs showing the microstructure of the Cu film after tensile straining at 10^{-4} /s. Inset in (a) is the corresponding selected area diffraction patterns, showing polycrystalline structure. (c) HRTEM image showing the DT tip of grain B in (a). Inset is the corresponding fast Fourier transform of the DTs and the inverse FFT HRTEM image of the DT tip containing stacking faults (SFs). (d) Magnified view of grain C in (b). (e) HRTEM image of the region containing the twins, and the 9R structure [boxed area in (d)] and its FFT (inset). (g) Magnified view of grain D in (f). (h) Inverse FFT HRTEM image of one end of the deformation twin, showing a wider ITB composed of PB1, 9R, and PB2 in grain D. Inset is the corresponding FFT of 9R. Grain boundaries of grains B and D are marked by the asterisks.

boundaries (PBs).^{16,17} It should be pointed out that in our as-deposited Cu films initial twins with 9R structure (or an incoherent twin boundary) are frequently observed in the large-sized grains ($> \sim 200$ nm), while in small-sized grains the two ends of most initial twins terminate at GBs.

III. RESULTS AND DISCUSSION

Figures 1 and 2 respectively show the presence of DTs in the Cu films stretched at 1×10^{-4} /s and 1×10^0 /s; e.g., ~ 45 -nm-sized grains A and B, ~ 110 -nm-sized grain C, and ~ 200 -nm-sized grains D and E contain multiple twins. The HRTEM images of grains B, C, and D are respectively shown in Figs. 1(c), 1(e), and 1(h), together with the corresponding fast Fourier transforms (FFTs) indicating the twinning relationship. These DTs have two types of twin boundary, $\Sigma 3\{111\}$ coherent twin boundaries and $\Sigma 3\{112\}$ incoherent twin boundaries. One can see that some DTs have two ends

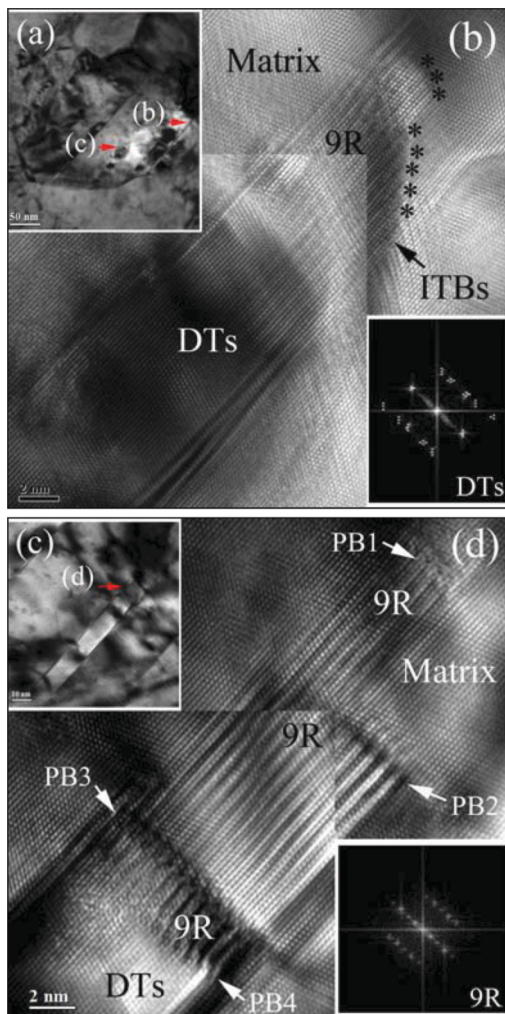


FIG. 2. (Color online) (a) 275-nm-sized grain containing multiple twins deformed at strain rate 1×10^{-4} /s. (b) HRTEM image of the front end of the twin indicated in (a). Inset is the corresponding FFT of the DTs. (c) Magnified view of twin ending in grain interior in (a). (d) HRTEM image of twin indicated in (c). Inset is the corresponding FFT of the 9R structure. A periodic array of defects is observed with a repeat unit of three $\{111\}$ planes in both (b) and (d).

at GBs or the surface and others have one end inside the grains, which is possibly associated with the nucleation of partials from the GB or surface dislocation source at this length scale.^{2,11,12,21,22} From the HRTEM observations, it is noted that in large-sized grains (i) a repeated pattern with periodicity of three times the interplanar spacing of $\Sigma 3\{111\}$ planes is clearly observed [Figs. 1(d), 1(h) and 2] and (ii) the 9R structure is bounded between the two PBs [see Figs. 1(h) and 2(d)]. Both the HRTEM observations and the corresponding FFT confirm that the ends of the twins are $\Sigma 3\{112\}$ incoherent twin boundaries. This supports the MD simulation results that incoherent twin boundaries can dissociate into two PBs, bounding a 9R phase, and that DTs can propagate with the front end as $\Sigma 3\{112\}$ incoherent twin boundaries.^{16,17} The deformation-induced 9R phase suggests that activation of the three ($b_2:b_1:b_3$) Shockley partials is highly cooperative (twinning dislocations successively or simultaneously glide either on adjacent or on separated $\{111\}$ atom planes),^{16–18} significantly distinct from the RAP mechanism⁵ via “one-after-another” glide of independent, single twinning partials on adjacent slip planes, in which the partials may be promoted layer by layer through reactions and cross slip.²³ Both Wang *et al.*¹⁷ and Li *et al.*¹⁸ pointed out that this particular CAP process can even entail synchronized activation of partials, i.e., simultaneous activation of three ($b_2:b_1:b_3$) Shockley partials as “zonal” twinning dislocations with different Burgers vectors, for coordinated slip on adjacent $\{111\}$ layers. The simultaneous passage of b_1 , b_2 , and b_3 in a single action is due to the highly cooperative and synchronized slip of only two partials (b_1 and b_2), while the surroundings are constrained to stay put, resulting in b_3 .¹⁸ Although such a two-layer-together cooperative shuffle is an effective way to relieve local concentration of high stresses, it would cost more energy than the slip of a single twinning partial carrying all layers above it,^{17,18} which renders the CAP mechanism (twinning dislocations successively or simultaneously glide on separated $\{111\}$ atom planes) is relatively easier to operate.²² This is consistent with the present TEM observations that most of the incoherent twin boundaries with a repeatable pattern involving many units of three $\{111\}$ atomic planes in large-sized grains. The existence of stacking faults in the 9R phase at the twin tip also indicates that the precondition for the nucleation of a deformation twin is to first activate a leading partial to create a stacking fault.^{9–12} In other words, a stacking fault was first formed by a leading partial, and then a twinning partial must be generated and follow the footsteps of the leading partial to convert the stacking fault to a twin nucleus. Another striking feature observed in Figs. 1(e) and 2(d) is the step structure of incoherent twin boundary with more than two PBs. This suggests that the CAP process is accomplished by the triplet unit partials ($b_2:b_1:b_3$) successively rather than simultaneously gliding on separated $\{111\}$ atom planes. It also suggests that the configuration of the GB can probably influence the nucleation of partials, disturbing the “infection” among the glide dislocations and stopping the twin (thickening or thinning) process.

In contrast, in small-sized grains, the ordered 9R phase was not frequently observed; instead stacking faults separated by four $\{111\}$ layers were found in the front tip of DTs, as indicated by arrows in Fig. 1(c). This is similar to the results

for deformed NC Ni with average grain size $D \sim 25$ nm.^{2,10} When the grain size is small, the global stress needed for plastic deformation must increase as well, causing a high local stress concentration. Although partial dislocations can readily be emitted from GBs to nucleate a deformation twin, it is statistically and practically impossible for a partial dislocation to exist on every slip plane to grow a single twin.²³ Nucleation of a new partial on every slip plane is difficult because of the required high energy. This is a possible reason for the formation of small-sized (three-layer) twins through the mechanism of synchronized activation of partials under extreme conditions, such as near the crack tip.^{18,24} In our case (at room temperature and low $\dot{\epsilon}$), the zero net macrostrain is probably caused by the RAP mechanism. Compared with the CAP process, the RAP twinning process would more effectively relieve the high local stress concentration at high $\dot{\epsilon}$ via random emission and gliding of partials, implying RAP twinning ought to be favored over the CAP twinning. The experimental observation⁵ that the fraction of RAP twins monotonically decreases with increasing $\dot{\epsilon}$ thus results from the suppression of CAP twin formation and the operation of other non-zero-strain twinning mechanism such as monotonic activation of partials at high $\dot{\epsilon}$.

Because DT is a perfectly coherent “stimulated slip” phenomenon,^{9,14} which is in contrast to the less coherent “spontaneous slip” of ordinary dislocation plasticity, uncorrelated emissions of individual partials cannot accidentally form a twin tens or even hundreds of atomic layers thick, like those seen in Figs. 1 and 2. The GB emissions of partial dislocations need to be spatially, and likely temporally, correlated. To thicken the twin via any ZSDT mechanism, the elastic compatibility and other requirements still demand that GB sites that can successfully promote stimulated slip are rather “special,”^{5,22} and the configurational density n_s of such sites should be proportional to the circumference of the slip plane–GB intersection, that is, $n_s \propto D$. Specifically, on a (111) plane in a Cu grain, the partial slip needs to be “promoted” to the next (111) plane, such that twinning dislocations become available on successive planes one after another in a highly correlated fashion to thicken the twin.^{9,14,22,23} To sustain this plane-to-plane “infection” required for stimulated slip, the partial moving on the (111) plane needs special GB sites where a twinning partial can be nucleated or created²² (for the CAP mechanism). Alternatively, the promotion could be achieved if the partials are emitted from certain GB sites where proper reactions occur to induce a suitable twinning partial on the next atomic plane²³ (for the RAP mechanism). In either case, this “promotion-to-the-next-layer” probability is

$$P_{\text{partials}}^{\text{promote}} = n_s P_{\text{mul}}^{\text{GB}} = k D P_{\text{mul}}^{\text{GB}}, \quad (1)$$

where n_s is the number of available GB sites with the right configurations and scales with the length of the perimeter of the (111) plane intersecting with the GB. $P_{\text{mul}}^{\text{GB}}$ is the probability to accomplish the multiplication of twinning partials, sustaining the dislocation “infection” (with the sequence of $b_2:b_1:b_3$) or reaction to successfully promote identical partial slip on next plane at the GB site, and k is a scaling constant. From Eq. (1), the smaller is D , the fewer proper sites are available, and the

less likely it is for the CAP ZSDT mechanism to switch on. For such small D , the RAP ZSDT mechanism can probably start,⁵ due to the change of GB configuration and increase in kinetic barriers accompanying the nucleation and glide of multiple twinning dislocations. Thus there exists a size effect in the ZSDT mechanism, which is verified by experimental observations (discussed below). If the grain size is extremely small such that there are no correct sites at the GBs to achieve the CAP and RAP processes, alternatively the mechanism of synchronized activation of partials can probably be switched on in the twinning process. Most recently, Ovid’ko²⁵ has suggested another approach that describes the formation of DTs through nanoscale multiplane shear, defined as an ideal shear occurring within a nanometer-sized volume. This approach is free from the assumption that some specific sites exist at GBs. However, the nanoscale ideal shear that occurs simultaneously along several neighboring crystal planes in crystals of infinite sizes can be triggered only at extremely high stress, even up to the ideal strength of materials. Once initiated, the nanoscale ideal shear can cause a change in configuration of the grain. This probably cannot happen in present experiments and does not contribute to the ZSDT.

Figures 3(a) and 3(b) display histograms, sorted for grains of different sizes, showing the number of grains containing DTs after deformation, for two strain rates. The nonmonotonic grain-size dependence of DT is demonstrated here at room temperature. From Figs. 3(a) and 3(b) one can clearly see that the maximum grain size that contains DTs (D_{max}) shifts from ~ 300 to ~ 220 nm and the fraction of DTs is reduced with decreasing $\dot{\epsilon}$. Generally, the tendency to form conventional DTs is very small at sizes of D larger than ~ 200 nm. However, the DT tendency then goes up when the grain size is reduced to below D_{max} , and it falls back down again with further reduction in the grain size. That means that an “inverse grain size” (D_{inv}) effect gradually takes over. We use a solid curve in the figures to represent the general trend of the DT behavior across the

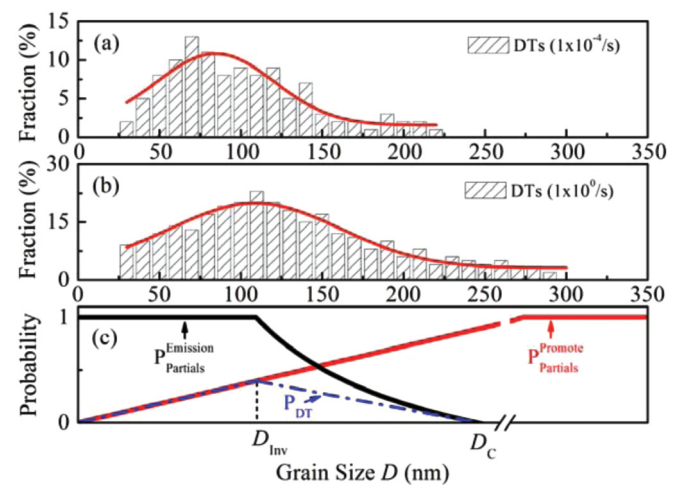


FIG. 3. (Color online) Grain-size effect on the formation of DTs in Cu thin films tensile tested at two strain rates, (a) 1×10^{-4} /s and (b) 1×10^0 /s. The solid line is a visual guide. (c) Schematic illustration of the D effects on the DT propensity P_{DT} , and its constituent $P_{\text{partial}}^{\text{emission}}$ and $P_{\text{partial}}^{\text{promote}}$ contributions, which lead to D_C and D_{inv} .

entire grain-size range studied, from which an apparent peak or saturation (probability 1) in twinning propensity is observed at D_{inv} . The error bar for the number of twinned grains, which are in double-digit numbers out of the ~ 100 grains we examined for each grain size, is believed to be much smaller than the difference seen in the figure for various grain sizes, so the peak observed appears to be real. Furthermore, DT is clearly more favorable at higher $\dot{\epsilon}$ as expected,^{1,2,9,10} and the inverse grain size D_{inv} moves from ~ 110 nm to lower grain size $D \sim 80$ nm as $\dot{\epsilon}$ is reduced, which is consistent with the results for NC Ni.¹⁰

As pointed out in our previous work,⁹ with grain size approaching the nanoscale, DTs can form via partial dislocations (including twinning partial dislocations) emitted from GBs.^{11,12} The probability of nucleating one such partial in lieu of the full dislocations scales with the difference in the required stresses ($\Delta\tau$),

$$\begin{aligned} P_{\text{partials}}^{\text{emission}} \propto \Delta\tau &= \tau_{\text{full}} - \tau_{\text{partial}} \\ &= \left(\frac{3m-1}{3} \frac{\mu b}{D} - \frac{\alpha-1}{\alpha} \frac{\gamma_{\text{sf}}}{b} \right) \\ &= \frac{\alpha-1}{\alpha} \frac{\gamma_{\text{sf}}}{b} \left(\frac{D_C}{D} - 1 \right), \end{aligned} \quad (2)$$

where μ is the shear modulus (48 GPa for Cu); γ_{sf} is the SFE (41 mJ/m² for Cu); the parameter α is the ratio of grain size to equilibrium stacking fault width;²⁶ m is a stress concentration factor (~ 4);⁴ and b is the magnitude of the Burgers vector of the full dislocation. There is a critical grain size D_C , which can be determined by setting Eq. (2) to zero ($D_C \sim 285$ nm for Cu, approaching the observed D_{max} at high $\dot{\epsilon}$) below which partial dislocation emissions dominate, leaving behind stacking faults and also setting the stage for subsequent DT. The switching on of this partial dislocation mechanism explains the fact that the fraction of stacking faults increases below D_C .^{9,10} However, as discussed above, the twinning dislocations become more

resistant to nucleation and slip with reducing grain size. If the grain size D is large enough (say, $1 \mu\text{m} > D_C$), the ZSDT mechanism will definitely operate via the CAP process, in which the partials are nucleated from the grain interior (similar to the observations⁶ in Ag). The two competing grain-size effects on the emission of the first partial dislocation and the plane-to-plane promotion of partial dislocation slip afterwards⁹ resulted in the double inverse grain-size effect on DT with respect to conventional Hall-Petch-type twinning behavior, as schematically illustrated in Fig. 3(c). The product of the two competing terms [Eqs. (1) and (2)] determines the overall P_{DT} [dashed line in Fig. 3(c)], which exhibits a behavior consistent with the double inverse grain-size dependence in the NC regime.

IV. CONCLUSION

The ZSDT mechanism is demonstrated here for submicron- and nano-sized Cu deformed in tension at room temperature and different strain rates. In the NC Cu, the ZSDT mechanism transitioned from the CAP to the RAP process with reduction in grain size. The grain-size-dependent ZSDT mechanism is explained by considering the emission of the first partial dislocation and the plane-to-plane promotion of partial dislocation slip afterwards. A high strain rate can promote the RAP process in the nonmonotonic twinning behavior observed in the NC grain-size regime.

ACKNOWLEDGMENTS

This work was supported by the National Natural Science Foundation of China (Grant Nos. 50971097, 51201123), the 973 Program of China (Grant No. 2010CB631003), and the 111 Project of China (Grant No. B06025). G.L. thanks the Fundamental Research Funds for the Central Universities for support. J.Y.Z. thanks China Postdoctoral Science Foundation funded project for part of financial support.

*Corresponding author: lgsammer@mail.xjtu.edu.cn

†Corresponding author: junsun@mail.xjtu.edu.cn

¹J. W. Christian and S. Mahajan, *Prog. Mater. Sci.* **39**, 1 (1995).

²Y. T. Zhu, X. Z. Liao, and X. L. Wu, *Prog. Mater. Sci.* **57**, 1 (2012).

³M. W. Chen, E. Ma, K. J. Hemker, H. W. Sheng, Y. M. Wang, and X. M. Cheng, *Science* **300**, 1275 (2003).

⁴C. X. Huang, K. Wang, S. D. Wu, Z. F. Zhang, G. Y. Li, and S. X. Li, *Acta Mater.* **54**, 655 (2006).

⁵X. L. Wu, X. Z. Liao, S. G. Srinivasan, F. Zhou, E. J. Lavernia, R. Z. Valiev, and Y. T. Zhu, *Phys. Rev. Lett.* **100**, 095701 (2008).

⁶L. Liu, J. Wang, S. K. Gong, and S. X. Mao, *Phys. Rev. Lett.* **106**, 175504 (2011).

⁷M. A. Meyers, O. Vohringer, and V. A. Lubarda, *Acta Mater.* **49**, 4025 (2001).

⁸M. A. Meyers, U. R. Andrade, and A. H. Chokshi, *Metall. Mater. Trans. A* **26**, 2881 (1995).

⁹J.-Y. Zhang, G. Liu, R. H. Wang, J. Li, J. Sun, and E. Ma, *Phys. Rev. B* **81**, 172104 (2010).

¹⁰X. L. Wu and Y. T. Zhu, *Phys. Rev. Lett.* **101**, 025503 (2008).

¹¹H. Van Swygenhoven, P. Derlet, and A. Froseth, *Acta Mater.* **54**, 1975 (2006).

¹²V. Yamakov, D. Wolf, S. R. Phillpot, A. K. Mukherjee, and H. Gleiter, *Nat. Mater.* **1**, 45 (2002).

¹³M. Niewczas and G. Saada, *Philos. Mag. A* **82**, 167 (2002).

¹⁴Q. Yu, Z. Shan, J. Li, X. Huang, L. Xiao, J. Sun, and E. Ma, *Nature (London)* **463**, 335 (2010).

¹⁵Y. T. Zhu, J. Narayan, J. P. Hirth, S. Mahajan, X. L. Wu, and X. Z. Liao, *Acta Mater.* **57**, 3763 (2009).

¹⁶J. Wang, O. Anderoglu, J. P. Hirth, A. Misra, and X. Zhang, *Appl. Phys. Lett.* **95**, 021908 (2009).

¹⁷J. Wang, N. Li, O. Anderoglu, X. Zhang, A. Misra, J. Y. Huang, and J. P. Hirth, *Acta Mater.* **58**, 2262 (2010).

¹⁸B. Q. Li, B. Li, Y. B. Wang, M. L. Sui, and E. Ma, *Scr. Mater.* **64**, 852 (2011).

¹⁹D. L. Medlin, G. H. Campbell, and C. B. Carter, *Acta Mater.* **46**, 5135 (1998).

²⁰D. L. Medlin, S. M. Foiles, and D. Cohen, *Acta Mater.* **49**, 3689 (2001).

- ²¹G. Dehm, *Prog. Mater. Sci.* **54**, 664 (2009).
- ²²Q. Yu, L. Qi, K. Chen, R. K. Mishra, J. Li, and A. M. Minor, *Nano Lett.* **12**, 887 (2012).
- ²³Y. T. Zhu, X. L. Wu, X. Z. Liao, J. Narayan, S. N. Mathaudhu, and L. J. Kecskés, *Appl. Phys. Lett.* **95**, 031909 (2009).
- ²⁴B. Q. Li, M. L. Sui, B. Li, E. Ma, and S. X. Mao, *Phys. Rev. Lett.* **102**, 205504 (2009).
- ²⁵I. A. Ovid'ko, *Appl. Phys. Lett.* **99**, 061907 (2011).
- ²⁶R. J. Asaro and S. Suresh, *Acta Mater.* **53**, 3369 (2005).